NASA Technical Memorandum 4783

The F/A-18 High-Angle-of-Attack Ground-to-Flight Correlation: Lessons Learned

Daniel W. Banks, David F. Fisher, Robert M. Hall,
Gary E. Erickson, Daniel G. Murri, Sue B. Grafton,
and William G. Sewall

January 1997

NASA Technical Memorandum 4783

The F/A-18 High-Angle-of-Attack Ground-to-Flight Correlation: Lessons Learned

Daniel W. Banks and David F. Fisher
Dryden Flight Research Center
Edwards, California

Robert M. Hall, Gary E. Erickson, Daniel G. Murri,
Sue B. Grafton, and William G. Sewall
NASA Langley Research Center
Hampton, Virginia

National Aeronautics and
Space Administration
Office of Management
Scientific and Technical
Information Program
1997

THE F/A-18 HIGH-ANGLE-OF-ATTACK GROUND-TO-FLIGHT CORRELATION: LESSONS LEARNED

Daniel W. Banks and David F. Fisher
NASA Dryden Flight Research Center
Edwards, California

Robert M. Hall, Gary E. Erickson, Daniel G. Murri,
Sue B. Grafton, and William G. Sewall
NASA Langley Research Center
Hampton, Virginia

ABSTRACT

Detailed wind tunnel and flight investigations were performed on the F/A-18 configuration to explore the causes of many high-angle-of-attack phenomena and resulting disparities between wind tunnel and flight results at these conditions. Obtaining accurate predictions of full-scale flight aerodynamics from wind-tunnel tests is important and becomes a challenge at high-angle-of-attack conditions where large areas of vortical flow interact. The F/A-18 airplane was one of the first high-performance aircraft to have an unrestricted angle-of-attack envelope, and as such the configuration displayed many unanticipated characteristics.

Results indicate that fixing forebody crossflow transition on models can result in a more accurate match of flow fields, and thus a more accurate prediction of aerodynamic characteristics of flight at high angles of attack. The wind tunnel results show that small geometry differences, specifically nosebooms and aft-end distortion, can have a pronounced effect at high angles of attack and must be modeled in sub-scale tests in order to obtain accurate correlations with flight.

NOMENCLATURE

All force, moment, and pressure data have been reduced to coefficient form. All longitudinal data are presented in the stability axis system, while all lateral-directional data are presented in the body axis system. Moment data are referred to a moment center located at 25% of the mean aerodynamic chord.

AR	aspect ratio
b	span, ft
b'	local span, ft

β	sideslip angle, deg
δ_f	flap deflection angle, deg
θ	circumferential angle, deg

INTRODUCTION

The design of high-performance fighter aircraft has always placed emphasis on maneuverability and agility. To this end the aerodynamic envelope of these aircraft has been expanded to include higher usable angles of attack. Significant separated and vortical flows develop over the aircraft at high angles of attack and may significantly interact. These types of flow fields result in nonlinear aerodynamics and cause significant changes in stability and control characteristics when compared with low angles of attack. The changes in stability and control at high angles of attack are difficult to predict from ground tests because of the varying sensitivities to test conditions such as Reynolds number and Mach number. It has been a goal of the NASA High-Angle-of-Attack Technology Program (HATP)[1] to develop a better understanding of these flow fields and their effect on ground-to-flight correlation.

Obtaining accurate wind-tunnel-to-flight correlation is a significant challenge. High-angle-of-attack conditions add a level of complexity to this already difficult task. In the end, a good understanding of the behavior of the associated flow fields and their potential interactions is necessary to produce useful design methodology and ground-test techniques that can accurately predict flight.

This paper reviews the results of the various wind tunnel and flight investigations of the F/A-18 configuration leading to a more comprehensive understanding of these disparities and more accurate ground-to-flight correlation at high-angle-of-attack conditions. The results reported herein were obtained from various wind tunnel tests of several 6%- and 16%-scale F/A-18 models, and flight tests of the F-18 High-Alpha Research Vehicle (HARV) conducted at the Dryden Flight Research Center, Edwards, California (DFRC).

BACKGROUND

The F/A-18 configuration, due to its interesting high-angle-of-attack characteristics, unrestricted angle-of-attack envelope, and the availability of a flight test aircraft and wind tunnel models, was adopted for much of the work of the HATP. Since the F/A-18 aircraft was one of the first aircraft capable of controlled flight at high angles of attack, it displayed many unusual characteristics that were not well understood during early high-angle-of-attack flight tests. The features of the F/A-18 aircraft that made it attractive for high-angle-of-attack research included its contoured wing-body leading-edge extensions (LEXs), and its forebody shape, which is approximately elliptical with the major axis in the vertical plane aft of the radome. The design of the F/A-18 aircraft

data, all leading- and trailing-edge flap positions were made consistent with the flight vehicle configuration at that flight condition. The configuration that was tested on the HARV at $\alpha \geq 26°$ and $M_\infty \leq 0.76$ was $\delta_{LE} = 33°$ and $\delta_{TE} = 0°$.

6% Models

There were two 6% model configurations that are reported herein. The first is referred to as the MD/Navy 6% model (fig. 1). This model is the 6% wind-tunnel model originally used by McDonnell Douglas (St. Louis, Missouri) and the U.S. Navy during the design and test of the F/A-18, which was tested in the current F/A-18 configuration. The second 6% model consisted of the back end of the MD/Navy 6% model with a more recently constructed and instrumented forebody section (from nose apex back to LEX/wing juncture). This forebody had pressure ports from the nose back to the mid LEX region and is referred to as the NASA 6% model (fig. 2). Thus, these two models/configurations shared the same wings, empennage, and support system hardware. The pressure instrumentation consisted of 440 pressure orifices distributed circumferentially at 5 stations on the nose and spanwise at 3 stations across the LEXs, as shown in figure 3. The pressures were measured by internally mounted electronic scanning pressure modules located within the forebody. The on-surface flow visualizations were obtained with a mixture of titanium dioxide (TiO_2), mineral oil, and a small amount of oleic acid added for dispersion.[14] The mixture was applied to the model, the tunnel was then brought on condition long enough for the mixture to set, and then rapidly brought to a static condition when photographic documentation was taken. The off-surface flow visualizations were obtained with water vapor (injected or natural) and a laser light sheet in the wind tunnel, this was recorded with video cameras.[15] The 6% model wind-tunnel

Figure 1. MD/Navy 6% F/A-18 model in the NASA Langley 7- × 10-ft High Speed Tunnel.

16% Models

There are two 16% low Reynolds number models reported herein. The first was modified from an older preproduction 16%-scale F/A-18 model configuration and although it was modified to more closely represent the F/A-18 configuration as it evolved, still incorporated some differences. Figure 4 shows this model and is called the NASA-1 16% F/A-18 model. There are limited flow visualization results presented here from this model. The second 16%-scale F/A-18 model represents the current F/A-18C configuration and was of much higher fidelity than the NASA-1 16%-scale model. This second F/A-18 model is referred to as the NASA-2 16% model and shown in figure 5. The NASA-2 16% model was also designed with more instrumentation than the NASA-1 16% model and all of the 6% models. Both 16% models were constructed of lightweight fiberglass since they were also used as free-flight models and therefore were limited to lower dynamic pressure than the 6% models. The NASA-2 16% model also included removable components; some that were instrumented to determine the flow field effects of having pressure port roughness effects, and others to assess changes in geometry (e.g. the noseboom). The results from the NASA-2 16% model will be used for all quantitative data (force, moment, and pressure distributions) since it had a higher degree of fidelity in both geometry and data, and because of its flexibility in replaceable components. The NASA-2 16% model had a more extensive number of surface pressure measurements than the instrumented NASA 6% model; however, only those which correspond to the fuselage stations of the NASA 6% model will be reported here (fig. 3). Both of the 16% wind tunnel models were tested in NASA Langley Research Center's 14- × 22-ft Subsonic Tunnel and 30- × 60-ft Tunnel. The on-surface flow visualization was obtained from tests of the NASA-1 16% model. The technique was essentially the same as described for the 6% model, with the exception of the mixture being thinner to accommodate the lower dynamic pressures.

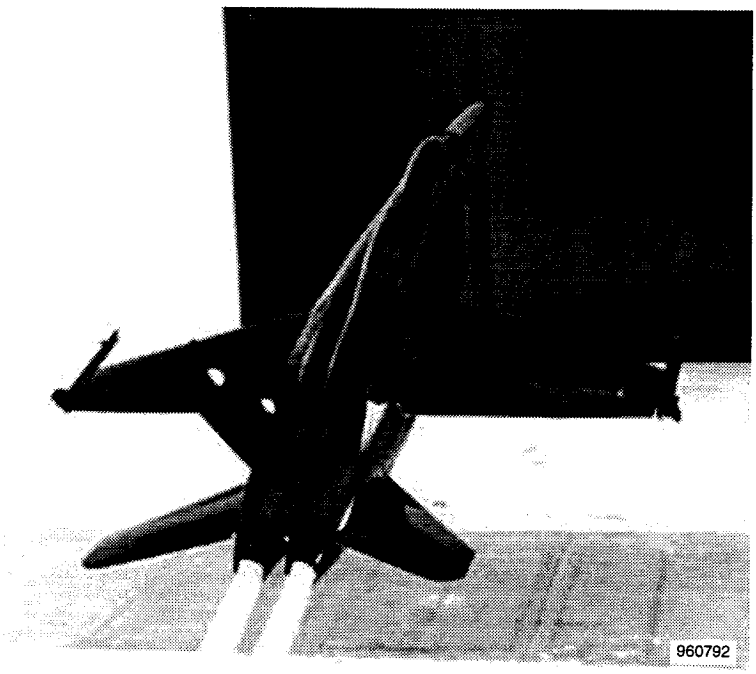

Figure 4. NASA-1 16% F/A-18 model in the NASA Langley 14- × 22-ft Subsonic Tunnel.

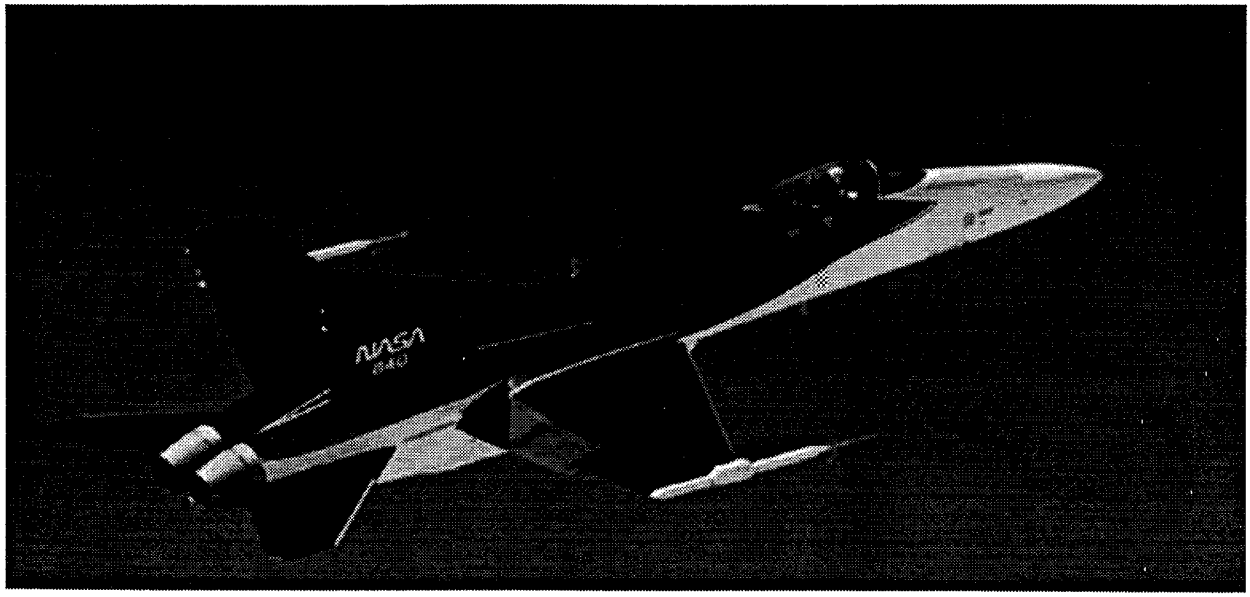

EC 88 0095-002

Figure 6. NASA HARV in flight at the NASA Dryden Flight Research Center, Edwards, California.

RESULTS AND DISCUSSION

Basic Aerodynamics

The basic longitudinal aerodynamic characteristics of the F/A-18 in the high-angle-of-attack configurations from wind tunnel tests are shown in figure 7. The longitudinal characteristics are similar between the models, with the major differences being small changes in $C_{L,max}$ and variations in pitching moment. Maximum lift occurs at approximately $\alpha = 40°$, with $C_{L,max} \sim$ 1.80. The NASA 6% model has greater pitch stability than the NASA-2 16% model at angles of attack from 25° to 40°, and greater nose down pitching moment from $\alpha = 10°$ to $\alpha = 45°$. Some effects of model geometry on this pitching moment difference will be discussed later in this report.

The lateral-directional characteristics of the NASA 6% and NASA-2 16% models in the high-angle-of-attack configuration at $\alpha = 40°$, are shown in figure 8. An angle of attack of 40° is of significant interest since this is the angle of attack for maximum lift. The NASA 6% model shows higher levels of lateral stability than the NASA-2 16% model at this angle of attack ($-4° \leq \beta \leq 4°$). The effects of Reynolds number, grit, and noseboom on lateral stability will be discussed later in the report.

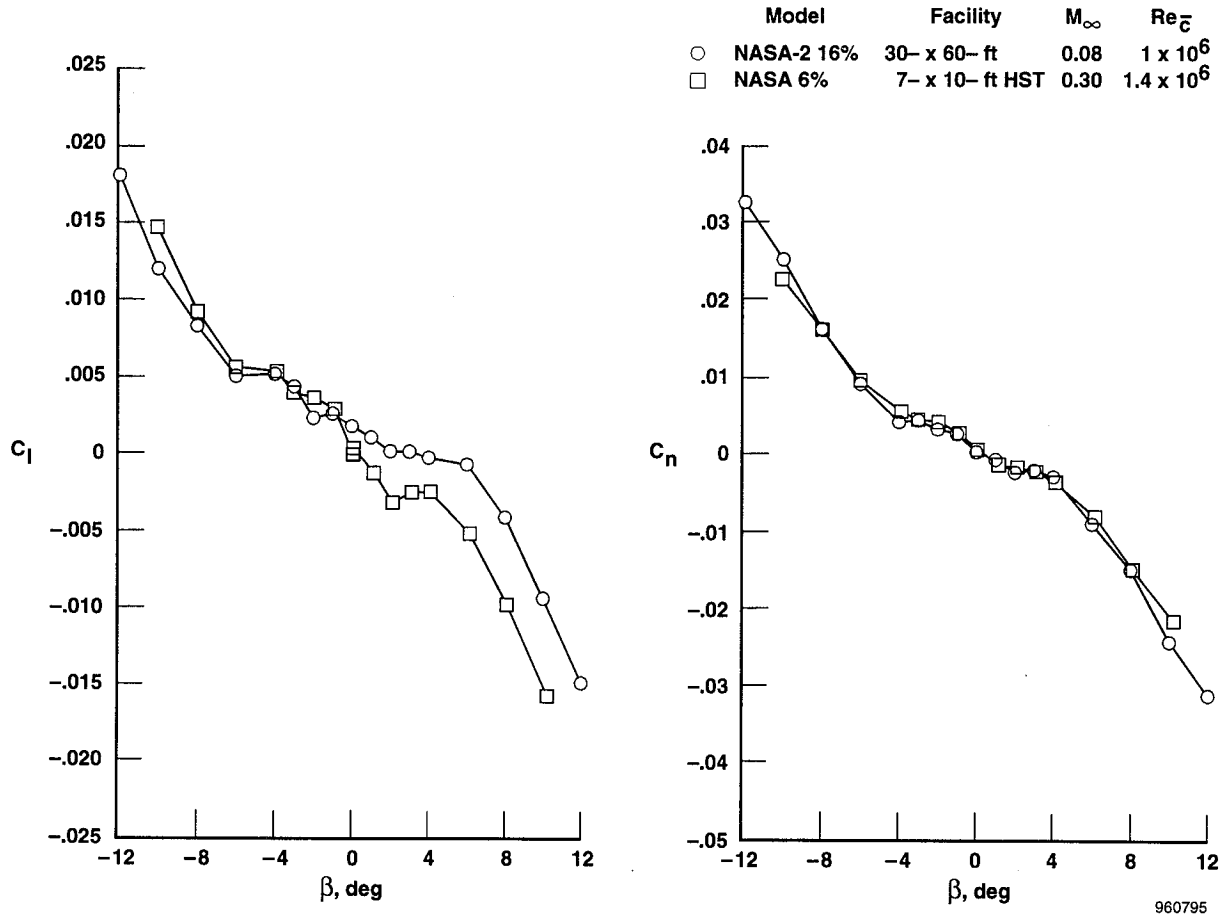

Figure 8. Lateral-directional aerodynamics of F/A-18 models. $\alpha = 40°$, $\delta_{fLE} = 33°$, $\delta_{fTE} = 0°$, $\delta_{HT} = -12°$.

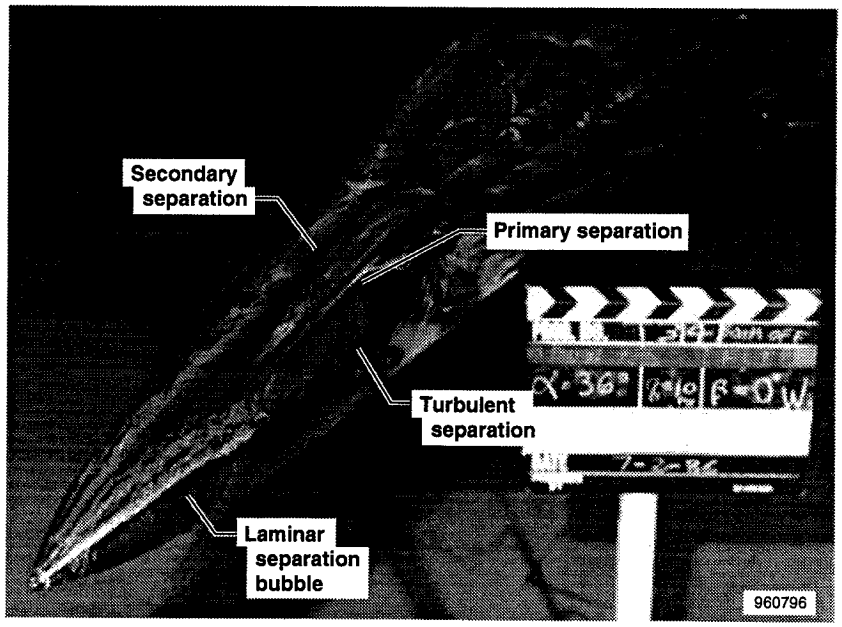

Figure 9. Forebody oil flow visualization of NASA-2 16% F/A-18 model. $\alpha = 36°$, $M_\infty = 0.08$, $Re_{\bar{c}} \sim 1 \times 10^6$.

dynamic pressure and to the viscosity effects of the oil on changing the local geometry. The MD/Navy 6% model was tested at a higher dynamic pressure and thus the oil mixture was somewhat more viscous, so the smaller model would also be more prone to local variations in geometry from the oil. The extent of transitional flow on the MD/Navy 6% forebody was more difficult to determine than the NASA-1 16% because of effects of the oil on the MD/Navy 6% model and the resultant patterns. However, it appears that the flow field present (extent of transitional flow) on the forebody of each model was different even though this visualization was obtained at nearly the same Reynolds number.

On-surface flow characteristics of the HARV at $\alpha = 34°$, and $M_\infty = 0.3$ are shown in figure 11. The HARV displays a similar surface topology to that of the models with some notable differences. The forebody flow of the HARV appears to be fully turbulent aft of the radome. There is a small run of laminar flow on the radome, but it has fully transitioned by FS 107.[8] Recall that the NASA-1 16% model showed a significant vortex structure pass over the canopy and the MD/Navy 6%, under some conditions, showed a similar although less defined vortex which did not propagate over the canopy. Although the HARV had no flow visualization on the canopy the secondary separation lines are well defined up to the canopy.

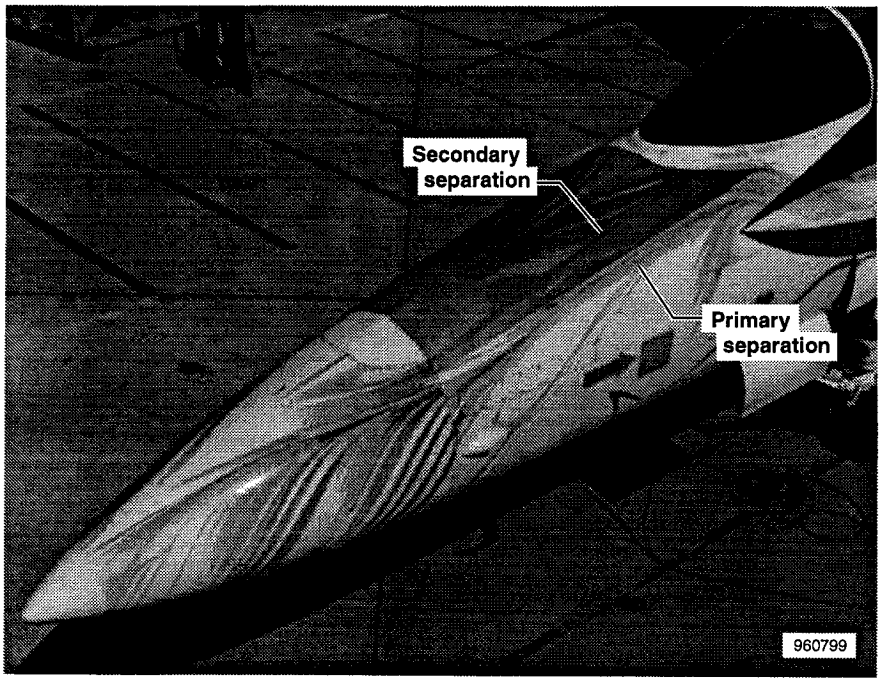

Figure 11. Forebody flow visualization of NASA HARV. $\alpha = 34°$, $M_\infty = 0.3$, $Re_{\bar{c}} \sim 8.5 \times 10^6$.

The off-surface flow visualization of the HARV at $\alpha = 39°$, and $M_\infty = 0.24$ is shown in figure 12. This flow visualization was obtained with smoke injection into the feeding sheet of the forebody vortex and natural condensation in the LEX vortex. The off-surface visualization (fig. 12) shows the vortices propagating over the canopy and interacting with the LEX vortex. It is presumed that this type of interaction is also present on the models at some conditions, but it appears not to be present at many of the conditions tested.

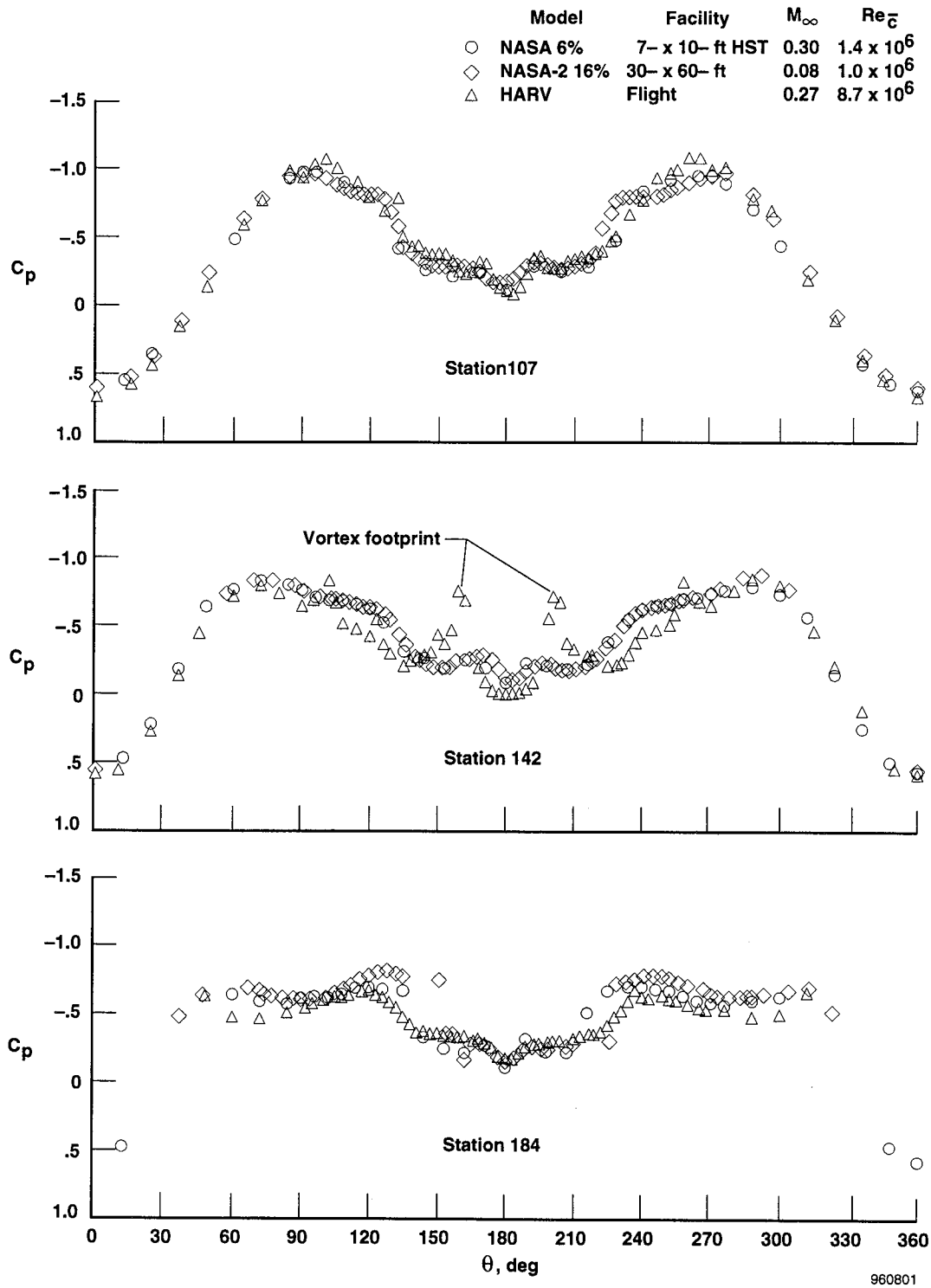

Figure 13. Forebody surface pressure distribution of F/A-18 models and HARV. $\alpha = 40°$.

and $M_\infty < 0.9$. At $M_\infty = 0.9$ there is no change in lateral stability from $M_\infty = 0.8$ and directional stability increases slightly for increasing angles of attack. At high angles of attack C_{l_β} is a stronger influence on departure resistance than is C_{n_β}, and it is typical for fighter-type configurations to have directional instability at high angles of attack. Gradual changes at lower Mach numbers are likely caused by locally transonic effects in the vortices. The large changes in C_{l_β} between $M_\infty = 0.6$ and $M_\infty = 0.7$ are most likely a result of the formation of local shocks on the wing and LEXs. In general the MD/Navy 6% model displays laterally stable behavior above $\alpha = 10°$ and through $M_\infty = 0.9$. This trend had typically been observed throughout the early development of the F/A-18 aircraft.

The forebody and LEX pressure distributions at various Mach numbers at $\alpha = 40°$ are shown in figures 15(a) and 15(b) respectively. The LEX pressure distributions were obtained in the David Taylor Research Center 7- × 10-ft Transonic Tunnel. There is a significant effect of Mach number on the LEX surface pressure distributions (fig. 15(b)). The LEX pressure distributions decrease and flatten out with increasing Mach number. The effects of Mach number on the LEX pressures are seen to persist below $M_\infty = 0.3$, typically the lower limit of significant compressibility effects. This is most likely caused by the high accelerations around the leading edge of the LEX resulting in local transonic flow. The effects on the forebody are less pronounced than the LEX. The forebody surface pressures are relatively insensitive to Mach number up to $M_\infty = 0.6$. The $M_\infty = 0.8$ data shows the suction peaks associated with the development of strong forebody vortices. This change at $M_\infty = 0.8$ is likely a result of shock induced separation on the forebody.

Effect of Reynolds Number and Forced Transition

Reynolds number effects on lifting surfaces have long been known to have a significant impact on model-to-flight correlations. As previously shown boundary-layer transition and therefore Reynolds number effects on forebody surfaces also have a significant effect on ground-to-flight correlations at high angles of attack. Forced transition techniques analogous to those developed for attached flows on wings and other surfaces[26] have been developed for forebodies at high angles of attack in conventional wind tunnels.[10] By properly transitioning the forebody boundary layer, simulating higher Reynolds numbers, and testing at the correct Mach number it is possible to more accurately predict flight results. The grit pattern that was used in the reported F/A-18 tests included a standard nosering, which has been used for conventional low/moderate angle-of-attack testing, and a so-called twin strip pattern shown in figure 16 in which two strips are placed longitudinally on both sides of the forebody approximately 54° from the windward attachment line.

The effects of a fully turbulent boundary layer on the surface flow characteristics of the NASA 6% model in the NASA Langley 7- × 10-ft High Speed Tunnel were assessed by adding additional TiO_2 particulates (to increase roughness) and testing at a higher dynamic pressure. The result is shown in figure 17 at $\alpha = 35°$ and $M_\infty = 0.5$, and many differences can be seen from that seen in figure 10. Recall figure 10 ($Re_{\bar{c}} = 1 \times 10^6$, $M_\infty = 0.22$) which showed very weak structure on the lee side of the forebody, the structures terminated at the LEX apex and did not pass over the canopy. Figure 17 now shows the strong vortex features on the forebody propagating over the canopy at $\alpha = 35°$ and $M_\infty = 0.5$ ($Re_d = 600{,}000$). Also the previously seen pooling and wedges

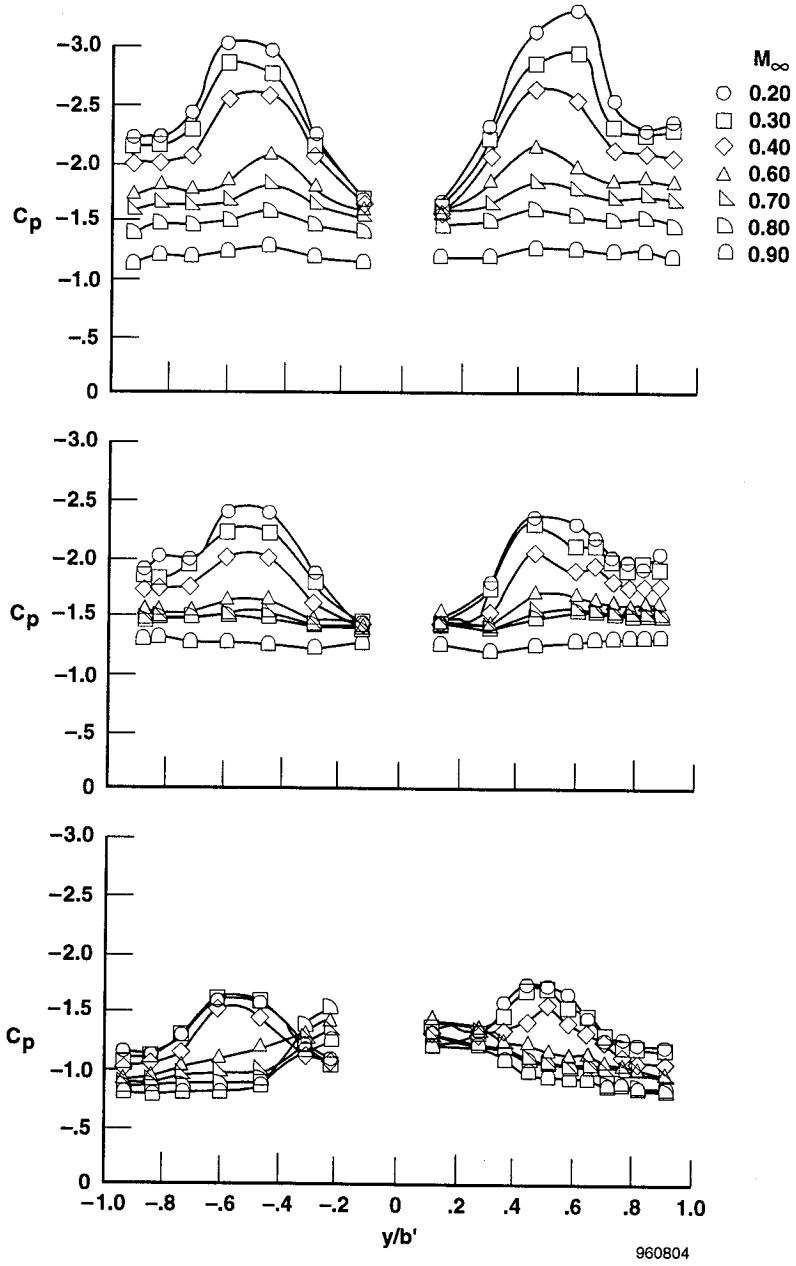

(b) LEX, upper surface.

Figure 15. Concluded.

At high angles of attack the local surface flow has a significant component in the cross-flow direction. Therefore, the twin strips are placed so that they transition each of the streamlines as they move around the body. Figure 18 shows the surface pressure distribution at fuselage stations 107, 142, and 184 with and without this fixed cross-flow transition at $\alpha = 36.4°$ and $M_\infty = 0.30$. The comparison shows that the major effect is the much more evident vortex footprints (suction peaks

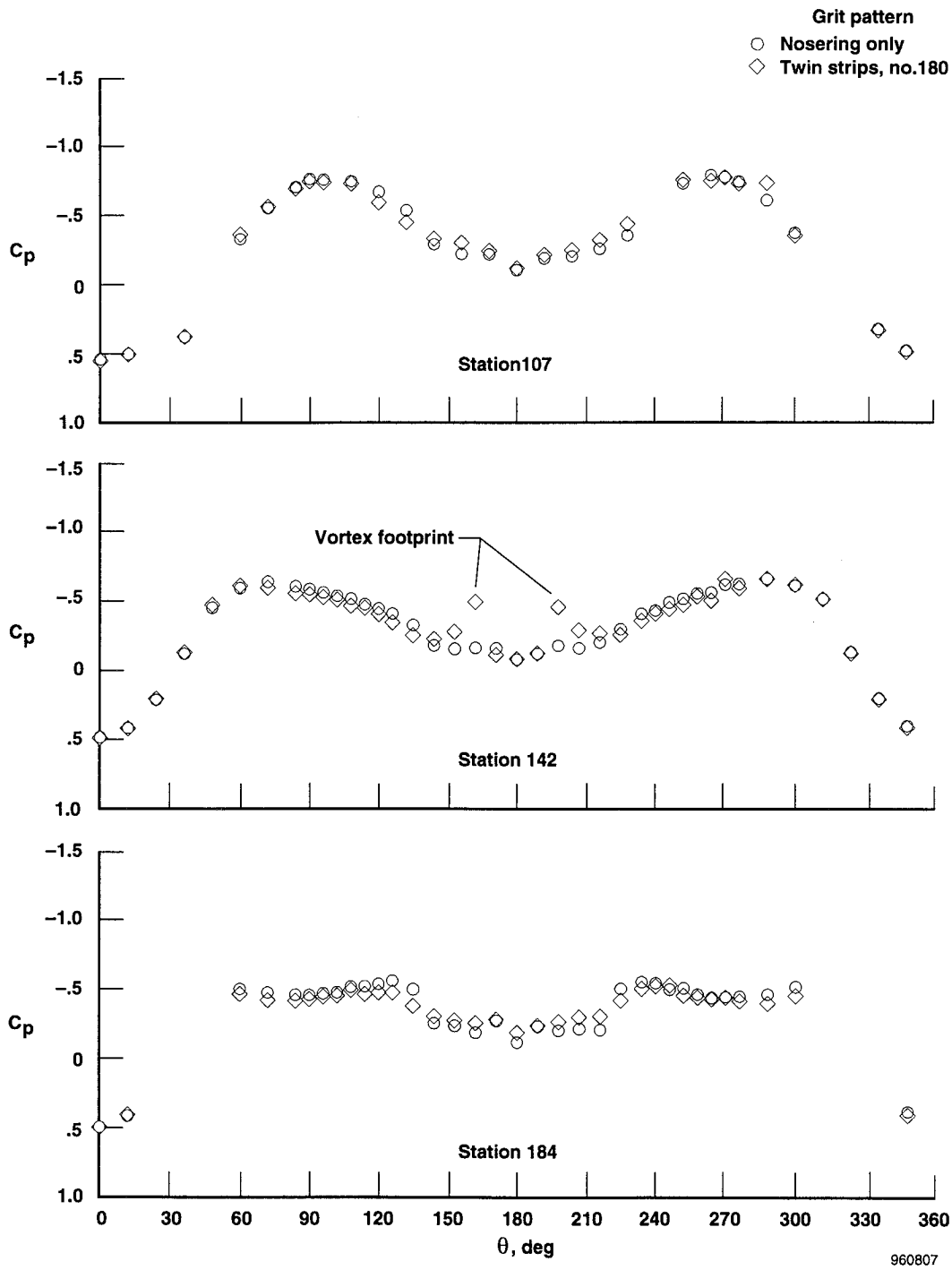

Figure 18. Effect of fixed transition on forebody pressure distribution of NASA 6% F/A-18 model. $\alpha = 36.4°$, $M_\infty = 0.3$, $Re_{\bar{c}} \sim 1.4 \times 10^6$.

Figure 20 shows the effect of fixed forebody cross-flow transition on the lateral-directional stability of the NASA 6% model at $\alpha = 36.4°$ and $M_\infty = 0.30$, with both 33° (fig. 20(a)) and 25° (fig. 20(b)) leading-edge flaps. Figure 21 shows the effects of fixed transition on the NASA-2 16% model at $\alpha = 40°$ and $M_\infty = 0.08$, with both 33° (fig. 21(a)) and 25° (fig. 21(b)) leading-edge flaps. At these conditions the predominant effect of the fixed forebody transition is to increase lateral stability ($-4° < \beta < 4°$). The direct effect of fixing crossflow transition is to increase the strength of the forebody vortices at high angles of attack. This indicates that, at least for the F/A-18, fixing transition in sub-scale tests has a favorable effect on the lateral stability when there is an interaction of the forebody vortices and the LEX flow field. This effect is more pronounced with the 25° leading-edge flap deflection than with the 34° deflection, probably because of the more separated and presumably weaker wing flow field with the 25° leading-edge flap deflection. In other words, with the 34° leading-edge flaps deflection the wing flow is much more attached and stronger and therefore more likely to resist the influence from the LEX vortices. The lateral stability changes with leading-edge flap deflection were much more pronounced with the NASA

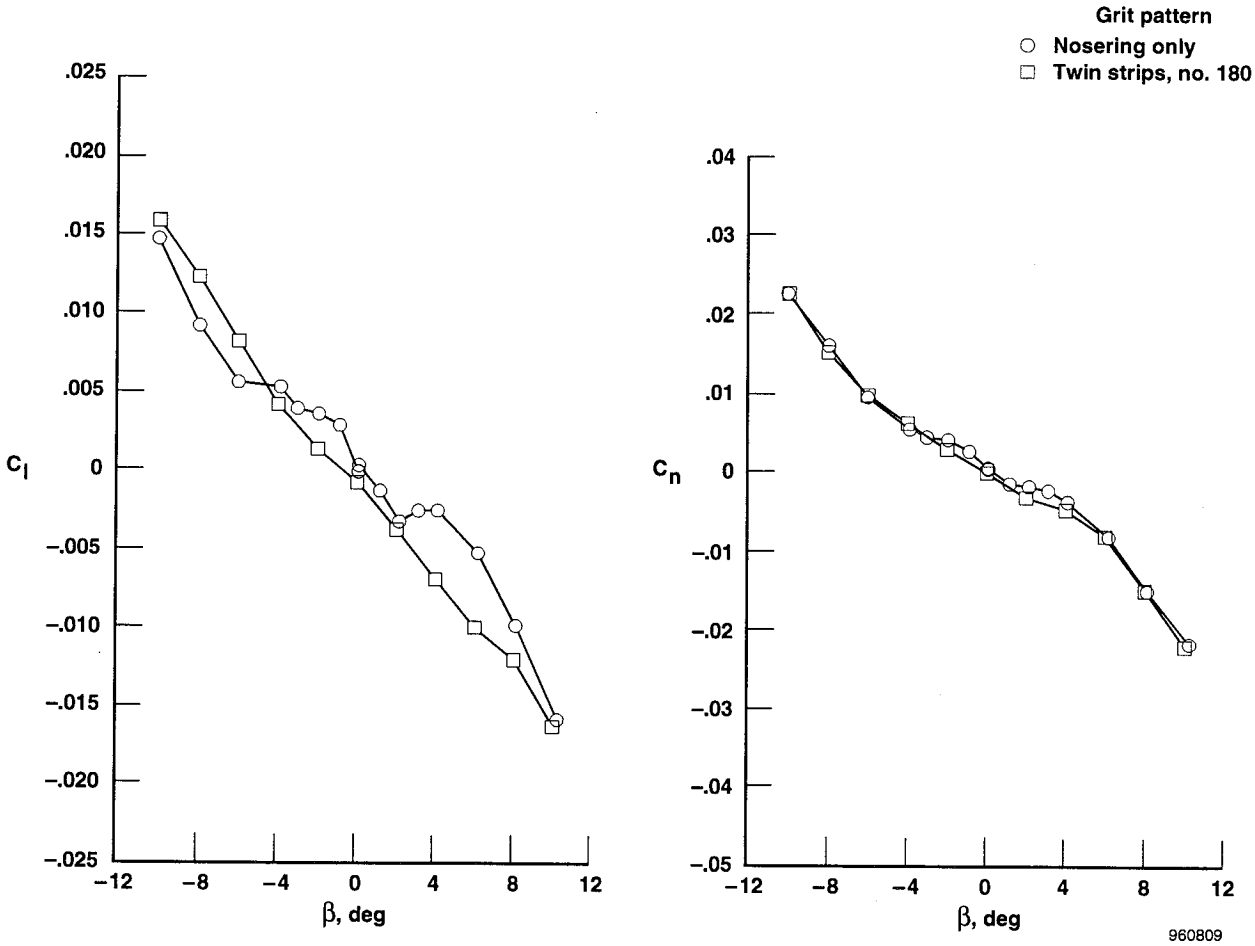

(a) $\delta_{fLE} = 33°$.

Figure 20. Effect of transition on lateral-directional stability of NASA 6% F/A-18 model. $\alpha = 36.4°$, $M_\infty = 0.3$, $Re_{\bar{c}} \sim 1.4 \times 10^6$.

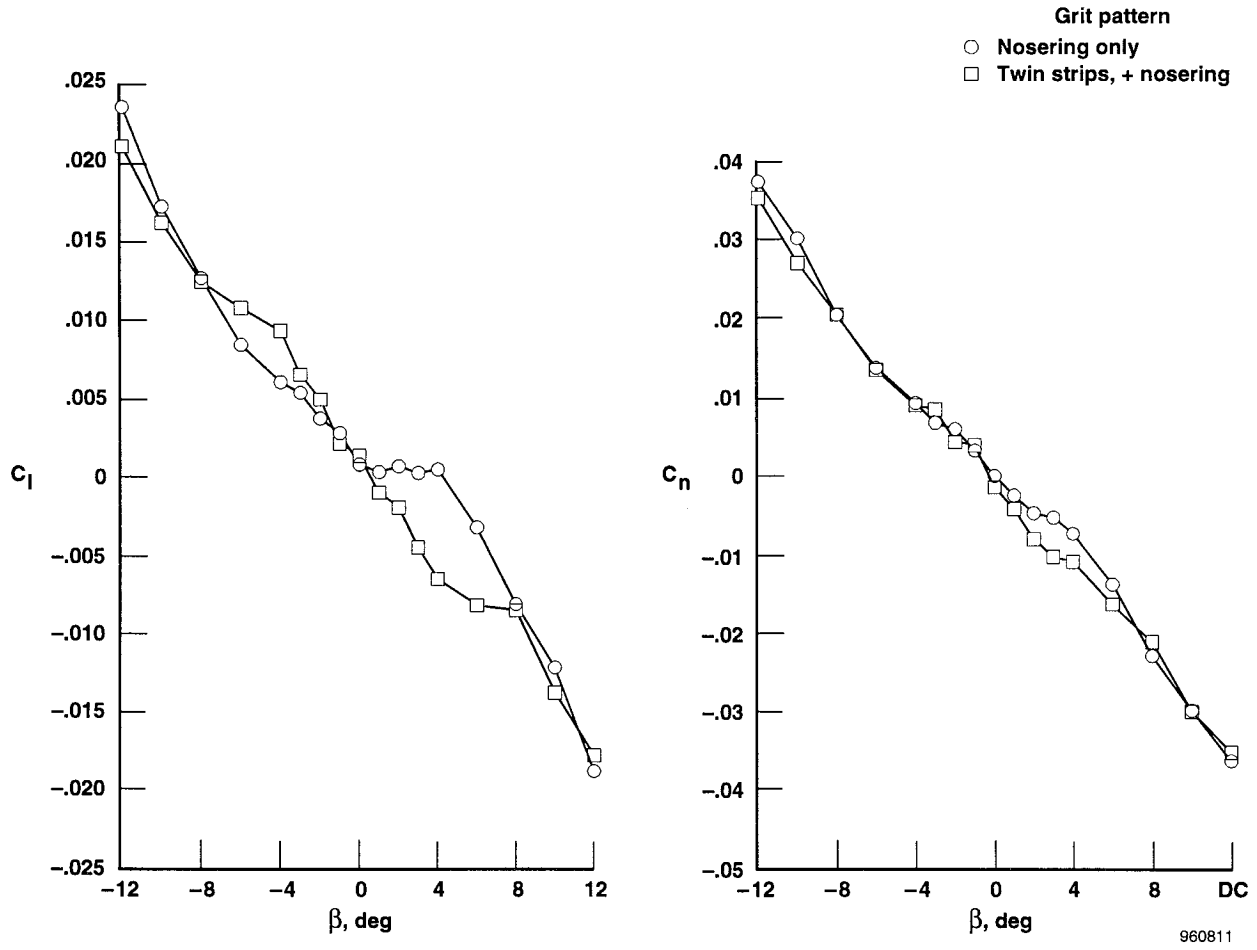

(a) $\delta_{fLE} = 33°$.

Figure 21. Effect of transition on lateral-directional stability of NASA-2 16% F/A-18 model. α = 40°, $M_\infty = 0.08$, $Re_{\bar{c}} \sim 1 \times 10^6$.

Geometry Effects

Geometry effects are an obvious area of concern for correlation between models and model to flight. Small geometry changes that have minimal impact at low angles of attack can have large and pronounced effects at high angles of attack. For sharp and high fineness ratio forebodies at high angles of attack, even small variations at the nose can change the vortex shedding and the subsequent flow field.[27] The ramifications for high-angle-of-attack testing is that geometric fidelity in the forebody region warrants serious attention. The conventional sensitivities for low/moderate angle-of-attack testing must still be taken into consideration.

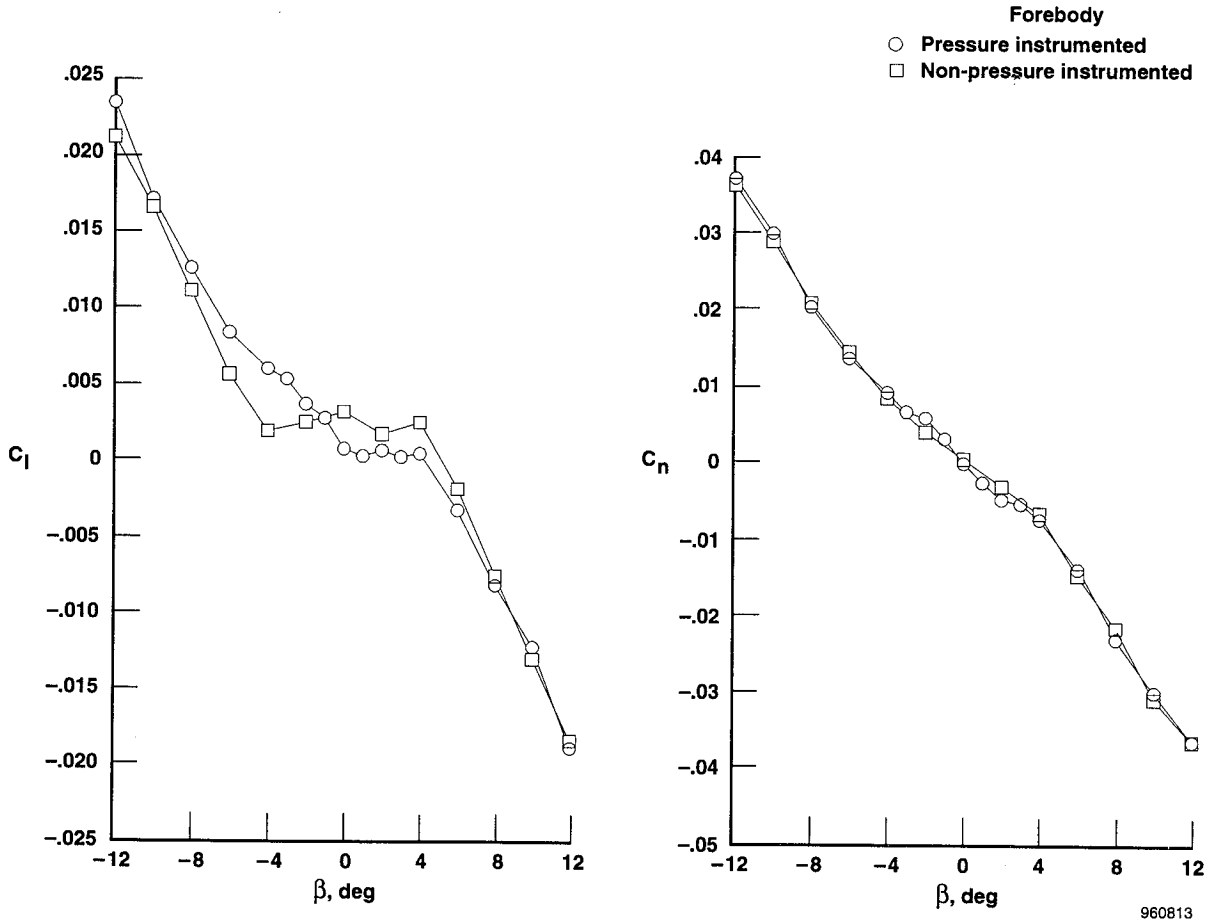

Figure 22. Effect of pressure ports on lateral-directional aerodynamics of NASA-2 16% F/A-18 model in the NASA Langley 30- × 60-ft Tunnel. $\alpha = 40°$, $M_\infty = 0.08$, $\delta_{fLE} = 33°$, $Re_{\bar{c}} \sim 1 \times 10^6$.

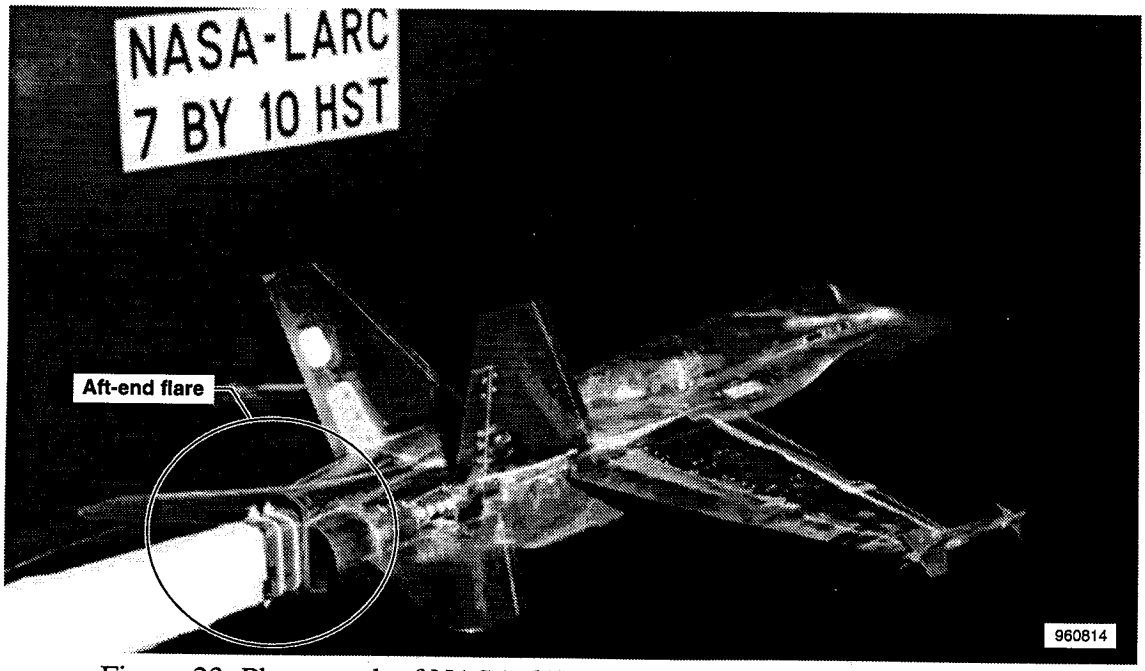

Figure 23. Photograph of NASA 6% F/A-18 model showing aft end flare.

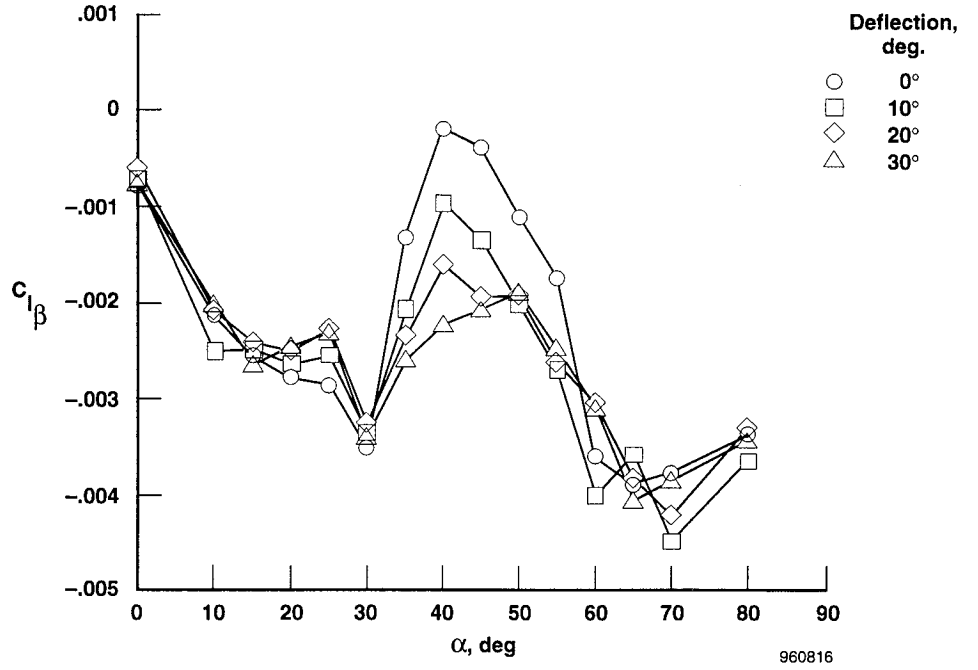

Figure 25. Effect of symmetric forebody strake deflections on lateral stability of the NASA-2 16% F/A-18 model. $M_\infty = 0.08$, $\delta_{fLE} = 33°$, $\delta_{fTE} = 0°$, $\Delta\beta = \pm 4°$, $Re_{\bar{c}} \sim 1 \times 10^6$.

Noseboom Effects

The effect of adding a noseboom on a configuration can be extremely significant. Subtle changes in the geometry near the tip of a sharp or high fineness ratio forebody, at high angles of attack, can have a dramatic effect on the separation about that forebody, and subsequently the forebody flow (vortices) and downstream interactions. The noseboom has the combined effect of changing the tip geometry, increasing the effective fineness ratio, and propagating its own wake. This effect can be seen in the laser vapor screen off-surface flow visualization shown in figure 26. This was

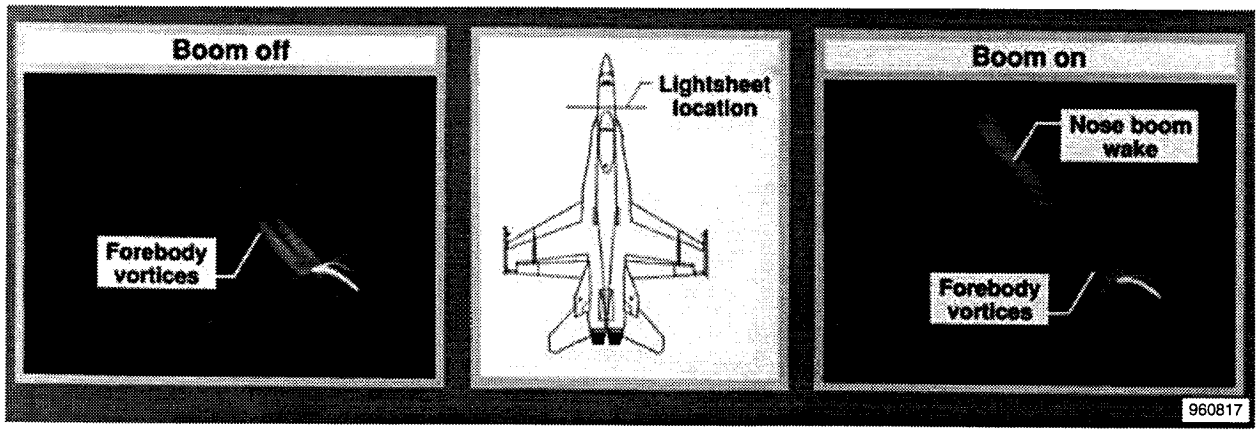

Figure 26. Flow visualization of NASA 6% F/A-18 forebody with and without noseboom. $\alpha = 50°$, $\beta = 0°$, $M_\infty = 0.6$, FS = 184. $Re_{\bar{c}} \sim 1.3 \times 10^6$.

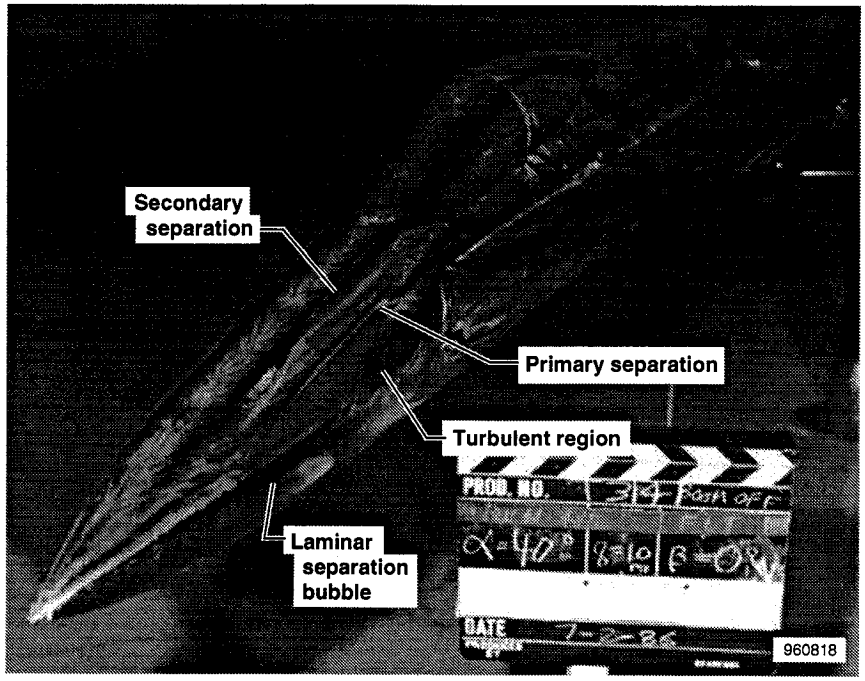

(a) Noseboom off.

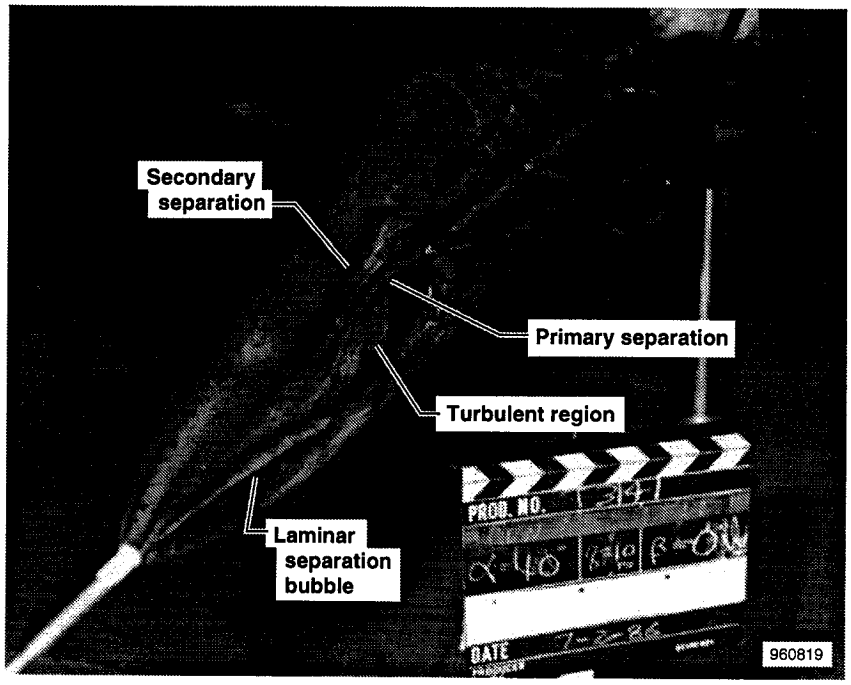

(b) Noseboom on.

Figure 27. Forebody flow visualization of NASA-2 16% F/A-18 model with and without noseboom. $\alpha = 40°$, $\beta = 0°$, $M_\infty = 0.08$, $Re_{\bar{c}} \sim 1 \times 10^6$.

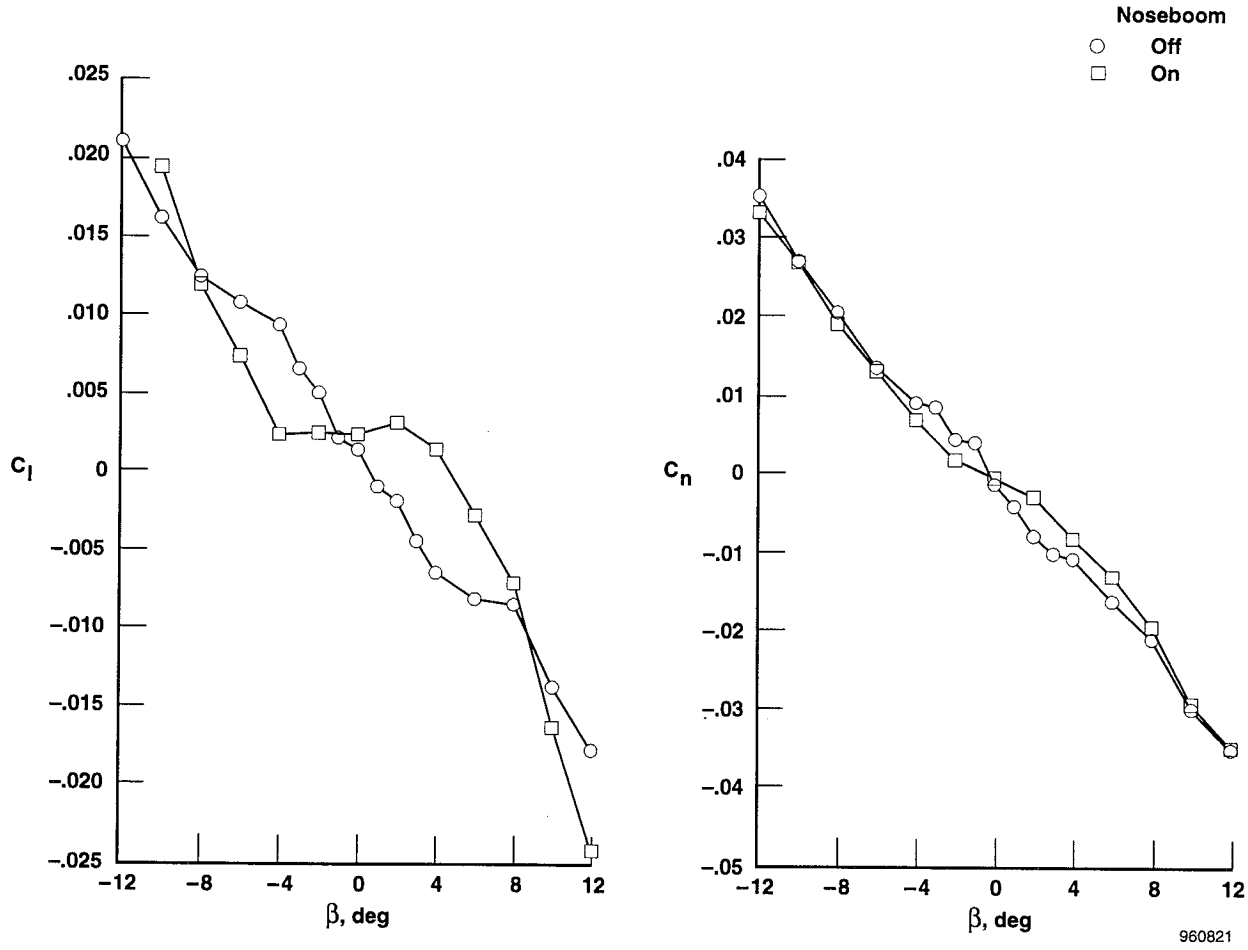

(a) $\delta_{fLE} = 33°$.

Figure 29. Effect of noseboom on lateral-directional aerodynamics of NASA-2 16% F/A-18 model. $\alpha = 40°$, $\beta = 0°$, $M_\infty = 0.08$, $Re_{\bar{c}} \sim 1 \times 10^6$, twin strips no. 36 grit.

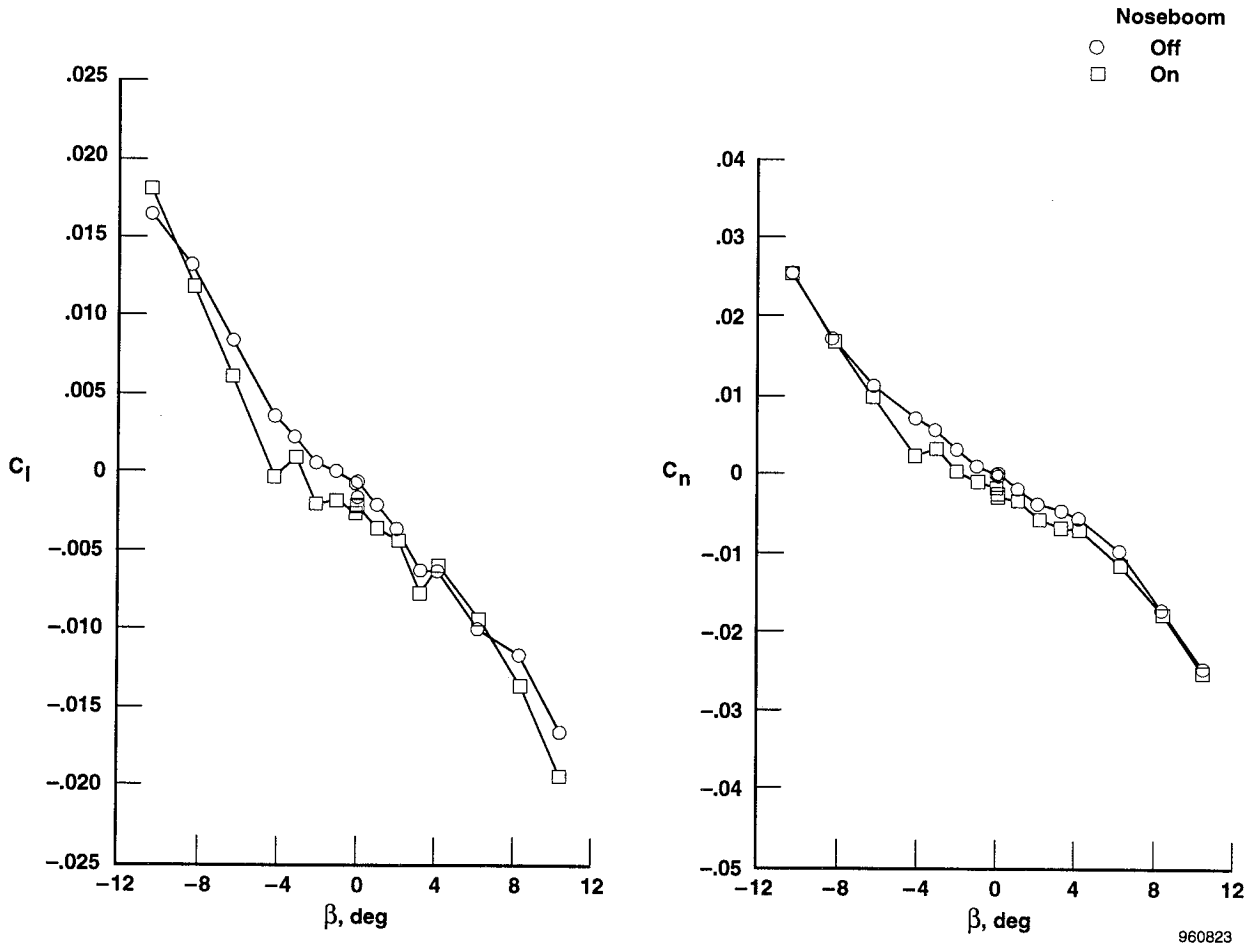

(a) $\delta_{fLE} = 33°$.

Figure 30. Effect of nose boom on lateral-directional aerodynamics of NASA 6% F/A-18 model. $\alpha = 37°$, $\beta = 0°$, $M_\infty = 0.3$, $Re_{\bar{c}} \sim 1.4 \times 10^6$, twin strips no. 180 grit.

Fixing transition can simulate higher forebody Reynolds numbers, and therefore provide better predictions of full-scale flight results from sub-scale wind tunnel tests. At high angles of attack it is necessary to fix crossflow transition on the forebody in addition to conventional transition fixing for lower angles of attack. The twin strip technique has been shown to be effective on the F/A-18 configuration.

Pressure ports and other subtle configuration differences can have a significant effect on the forebody flow field, and on the overall configuration flow field. The effect of pressure ports is to add roughness similar to grit. These are more apparent at high angles of attack where the forebody flow field becomes more significant.

Geometric differences can often have pronounced effects at high angles of attack. Aft end distortions, due to wind tunnel support, on some F/A-18 models resulted in increased nose down pitching moments compared to the undistorted geometry. Symmetric forebody strakes can have a significant effect on the forebody vortices and increase lateral stability of the F/A-18 at angles of attack near that of maximum lift. Nose probes or other protuberances on the forebody, especially near the tip, have a significant influence on the forebody flow field. These influences can reduce forebody vortex strength at high angles of attack and cause a reduction in lateral stability on the F/A-18. Increasing leading-edge flap deflection at high angles of attack decreases wing flow separation and reduces the effects of upstream influences; that is the LEX and forebody vortex flows in the case of the F/A-18. The combined effect of the nose probe and reduced leading-edge flap deflection can result in lateral instability at angles of attack near maximum lift for the F/A-18.

REFERENCES

[1]Gilbert, William P. and Gatlin, Donald H., "Review of the NASA High-Alpha Technology Program," *High-Angle-of-Attack Technology Conference*, NASA CR-3149, pt. 1, vol. 1, Oct. 30–Nov. 1, 1992, pp. 23–59.

[2]Lee, B.H.K., Brown, D., Zgela, M., and Poirel, D., "Wind Tunnel Investigation and Flight Tests of Tail Buffet on the CF-18 Aircraft," *AGARD Specialists' Meeting on Aircraft Loads due to Flow Separation*, Sorrento, Italy, Apr. 1–6, 1990.

[3]Meyn, L.A. and James, K.D., "Full-Scale Wind Tunnel Studies of F/A-18 Tail Buffet," AIAA-93-3519, Monterey, CA, 1993.

[4]Meyn, L.A., James, K.D., and Geenen, R.J., *Correlation of F/A-18 Tail Buffet Results*, NASA CP 10143, Fourth High Alpha Conference, NASA Dryden Flight Research Center, Edwards, CA, July 12–14, 1994.

[5]Shah, Gautam H., Grafton, Sue B., Guynn, Mark D., Brandon, Jay M., Dansberry, Bryan E., and Patel, Suresh R., "Effect of Vortex Flow Characteristics on Tail Buffet and High-Angle-of-Attack Aerodynamics of a Twin-Tail Fighter Configuration," presented at *NASA High-Angle-of-Attack Technology Conference*, NASA Langley Research Center, Hampton, Virginia, Oct. 30 –Nov. 1, 1990.

REPORT DOCUMENTATION PAGE

Form Approved
OMB No. 0704-0188

1. AGENCY USE ONLY (Leave blank)	2. REPORT DATE	3. REPORT TYPE AND DATES COVERED
	January 1997	Technical Memorandum

4. TITLE AND SUBTITLE

The F/A-18 High-Angle-of-Attack Ground-to-Flight Correlation: Lessons Learned

5. FUNDING NUMBERS

WU 505-68-30

6. AUTHOR(S)

Daniel W. Banks, David F. Fisher, Robert M. Hall, Gary E. Erickson, Daniel G. Murri, Sue B. Grafton, and William G. Sewall

7. PERFORMING ORGANIZATION NAME(S) AND ADDRESS(ES)

NASA Dryden Flight Research Center
P.O. Box 273
Edwards, California 93523-0273

8. PERFORMING ORGANIZATION REPORT NUMBER

H-2149

9. SPONSORING/MONITORING AGENCY NAME(S) AND ADDRESS(ES)

National Aeronautics and Space Administration
Washington, DC 20546-0001

10. SPONSORING/MONITORING AGENCY REPORT NUMBER

NASA TM-4783

11. SUPPLEMENTARY NOTES

Presented at NASA Langley High-Angle-of-Attack Technology Conference, Langley Research Center, Hampton, Virginia, September 17–19, 1996. Daniel Banks and David Fisher, Dryden Flight Research Center, Edwards, CA; Robert Hall, Gary Erickson, Daniel Murri, Sue Grafton, and William Sewall, NASA Langley Research Center, Hampton, VA.

12a. DISTRIBUTION/AVAILABILITY STATEMENT

Unclassified—Unlimited
Subject Category 02

12b. DISTRIBUTION CODE

13. ABSTRACT (Maximum 200 words)

Detailed wind tunnel and flight investigations were performed on the F/A-18 configuration to explore the causes of many high-angle-of-attack phenomena and resulting disparities between wind tunnel and flight results at these conditions. Obtaining accurate predictions of full-scale flight aerodynamics from wind-tunnel tests is important and becomes a challenge at high-angle-of-attack conditions where large areas of vortical flow interact. The F/A-18 airplane was one of the first high-performance aircraft to have an unrestricted angle-of-attack envelope, and as such the configuration displayed many unanticipated characteristics.

Results indicate that fixing forebody crossflow transition on models can result in a more accurate match of flow fields, and thus a more accurate prediction of aerodynamic characteristics of flight at high angles of attack. The wind tunnel results show that small geometry differences, specifically nosebooms and aft-end distortion, can have a pronounced effect at high angles of attack and must be modeled in sub-scale tests in order to obtain accurate correlations with flight.

14. SUBJECT TERMS

Fighter aircraft; Forebody flows; High angle of attack; Vortex flows; Vortex interactions

15. NUMBER OF PAGES

43

16. PRICE CODE

AO3

17. SECURITY CLASSIFICATION OF REPORT	18. SECURITY CLASSIFICATION OF THIS PAGE	19. SECURITY CLASSIFICATION OF ABSTRACT	20. LIMITATION OF ABSTRACT
Unclassified	Unclassified	Unclassified	Unlimited